ELSEVIER

Thermochimica Acta 387 (2002) 75–93

thermochimica acta

www.elsevier.com/locate/tca

An introduction to temperature modulated differential scanning calorimetry (TMDSC): a relatively non-mathematical approach

Zhong Jiang[a], Corrie T. Imrie[a], John M. Hutchinson[b,*]

[a]*Department of Chemistry, University of Aberdeen, Meston Walk, Aberdeen AB24 3UE, Scotland, UK*
[b]*Department of Engineering, University of Aberdeen, Meston Walk, Aberdeen AB24 3UE, Scotland, UK*

Received 15 October 2001; accepted 24 October 2001

Abstract

The purpose of this paper is a rather general overview of the principles of temperature modulated differential scanning calorimetry (TMDSC). The technique is compared to conventional DSC, and particular attention is paid to whether or not the heat flow in TMDSC may be separated into so-called thermodynamic and kinetic components. It is shown that in general it is not valid to make such a separation, and that in some cases to do so may lead to confusion. The problem of applying TMDSC in transition regions is considered in the light of the need to maintain a *quasi*-constant structure within any one modulation period, for which a knowledge of the molecular timescale is required. The view presented here is that either this is not normally known ''a priori'' or it must be deduced from an appropriate kinetic theory, and hence that the technique of TMDSC will always suffer from this limitation. © 2002 Elsevier Science B.V. All rights reserved.

Keywords: Temperature modulated differential scanning calorimetry

1. Introduction

Differential scanning calorimetry is the most widely used thermal analytical technique and finds application in areas ranging from pharmaceuticals through the food and chemical industries to fundamental physics. As we will see, DSC involves heating or cooling a sample at a constant rate and is most commonly used to detect phase transitions and to measure the associated thermodynamic properties such as temperature, heat capacity, and enthalpy changes. It became firmly established as a technique in the sixties and remained essentially unchanged for almost three decades. This situation changed abruptly in the early nineties with the commercial development of temperature modulated differential scanning calorimetry [1], though it was first described by Gobrecht et al. [2] some 20 years earlier.

The basic principle of temperature modulated differential scanning calorimetry (TMDSC) can be stated simply: in TMDSC, the constant rate of increase (or decrease) of temperature that is used in conventional differential scanning calorimetry (DSC) is modulated by superimposing upon it a periodic temperature modulation (often sinusoidal but not necessarily so) of a certain amplitude and frequency (or period). The effect is to introduce simultaneously to the experiment two different time scales: a long time scale corresponding to the underlying heating rate, and a shorter time scale corresponding to the period of the modulation.

The comparison of time scales corresponding to an underlying heating rate and to a period of modulation

* Corresponding author. Tel.: +44-1224-272820; fax: +44-1224-272497.
E-mail address: j.m.hutchinson@eng.abdn.ac.uk (J.M. Hutchinson).

0040-6031/02/$ – see front matter © 2002 Elsevier Science B.V. All rights reserved.
PII: S0040-6031(01)00829-2

may require some further explanation. The underlying heating rate is applied to the sample from an initial temperature for the scan until the final required temperature is reached. The response of the sample throughout is the superposition of all the kinetic responses, activated in various transition regions, and which have delays characterised by their relaxation times. If we consider an experiment in which the sample is heated from 25 to 125 °C at an underlying heating rate of 2 °C min^{-1} then the measurement time is 50 min. We would expect to detect molecular motions with relaxation times up to 50 min. Thus, the time scale corresponding to the underlying heating rate is ill-defined, but is certainly long. In contrast, each modulation starts anew at the end of every period, and only those molecular motions with relaxation times of the order of the period, which typically may be 60 s, or shorter will have time to make a contribution to the response. The advantages of this separation of time scales will be considered later after the essential features of conventional DSC have been reviewed.

The development of commercial TMDSC systems in the early 1990s heralded what many people believed to be a major advance in thermal analytical techniques, and in particular was considered as offering significant advantages over conventional DSC. Unfortunately, the situation that developed was rather more complicated than had originally been supposed, and the anticipated advantages of TMDSC are now by no means universally acknowledged. In part, this uncertainty has been due to the wide variety of commercial equipment that became available, including alternating DSC (ADSC, Mettler Toledo), Modulated DSC (MDSC, TA Instruments), Dynamic DSC (DDSC, Perkin-Elmer) and Oscillating DSC (ODSC, Seiko Instruments), each of which offered slightly different modulated temperature profiles and/or slightly different procedures for analysis of the data. This latter point is particularly important, with a debate still continuing over the relative merits of the two procedures: the reversing and non-reversing heat flow approach and the complex heat capacity approach, each of which is described in detail later.

In part also, TMDSC does not seem (at least to the present authors) to have achieved its anticipated potential as a result of a lack of understanding of the response of materials to the complex temperature histories involved. This applies especially to first-order phase transitions, most notably melting. Indeed, such transitions, which are often rather sharp, can introduce artefacts due simply to the inability to accommodate sufficient modulation periods within the transition. Finally, TMDSC suffers from the problem of heat transfer, which severely limits the range of variables that can be used, and which introduces additional artefacts in the heat flow. Of course, heat transfer problems are intrinsic to any calorimetric measurement, including conventional DSC. In the case of TMDSC, however, this presents a particular problem in view of the range of heating/cooling rates involved in any one experiment.

It will be appreciated from this brief resume that the use of TMDSC as a thermal analysis tool should be considered with caution, and that the interpretation of the numerous different output signals should only be undertaken with a good understanding of the background. There are several excellent reviews of TMDSC in the literature (e.g. [3,4]), but all of these are rather rigorous in their approach, requiring the reader to possess a strong mathematical background. The following discussion, therefore, is an attempt to highlight in a non-mathematical manner the important aspects users must consider when both designing TMDSC experiments and interpreting the resulting data.

2. DSC and TMDSC: the techniques

2.1. DSC

Conventional DSC, available now for several decades as a standard thermal analysis procedure, requires a sample, typically of the order of 10 mg mass, to be heated (or cooled) at a constant rate, typically of the order of 10 K min^{-1}, through a temperature range encompassing any transitions of interest. Commercial DSCs fall into two types. In power-compensated DSC the measured quantity is the difference in power between sample and reference required to maintain the sample and reference at the same temperature. In a heat flux instrument, it is the temperature difference between sample and reference which is measured as the reference is heated at the required rate; this temperature difference is then converted to a heat

flow by means of the appropriate conversion factor. For many years there was intense debate over the relative merits of these calorimeter designs but it is now accepted that the data obtained from the two are indistinguishable, though power compensation seems to have some advantages regarding the accuracy of absolute heat capacity measurements.

Heat transfer plays an important role in both types of instrument, and imposes certain constraints. For example, the larger the sample mass, the greater will be the heat flow signal for a given heating rate. On the other hand, the larger is the sample, the more non-uniform will be the sample temperature, and the greater will be the temperature lag between average sample temperature and programmed temperature. Thus, the choice of sample mass is a compromise between maximising the heat flow signal and minimising the thermal lag.

Likewise, the choice of heating rate is limited. A fast heating rate will provide a large heat flow signal, but with significant thermal lag between sample and programmed temperatures. In contrast, a slow heating rate will allow time for the sample to follow the programmed temperature closely, but will give a small heat flow signal. Again a compromise is called for. The heating rate also introduces the distinction between ''sensitivity'' and ''resolution''. The sensitivity is a measure of the ability to detect small heat flows, resulting for example from weak transitions, and is a function of the design and construction of the calorimeter. However, because the heat flow signal increases with heating rate, the sensitivity of any measurement can be improved by heating at a faster rate. On the other hand, the resolution is a measure of the ability to resolve a transition in respect of the temperature interval in which it occurs. This is improved by heating at a slower rate, which not only reduces the problem of thermal lag and temperature gradients, but also allows more time, within any given temperature increment, during which the heat flow from any thermal event may be recorded.

Allowance can be made for the temperature difference between sample and programmed temperature, for any heating rate, by calibrating the temperature scale using a pure calibrant (e.g. indium) with a sharp and well-known transition temperature (e.g. melting temperature of indium = 156.6 °C). It is assumed here that the sample, when scanned in the DSC at the calibrated heating rate, is at a uniform temperature: this will be an increasingly poor assumption as the heating rate increases and as the thermal conductivity of the sample material decreases. This calibration procedure is nearly always made on heating, because the problem of undercooling (or supercooling) on cooling at a constant rate does not easily permit the precise definition of a transition temperature, though this problem seems to have been solved recently [5]. Consequently, DSC scans are, strictly speaking, calibrated for heating only. Cooling scans are often of interest, however, because undercooling a transition can reveal thermodynamically metastable phases, such as monotropic liquid crystal phases.

The heat flow signal from the DSC will be composed of two parts: one is the heat flow required to raise the sample temperature at the programmed rate, and is directly related to the intrinsic heat capacity of the sample, and the other is the heat flow arising from kinetic processes that may occur during the heating scan, for example phase changes such as melting and crystallisation, liquid crystalline transitions or second order transitions such as the glass transition and its associated enthalpy relaxation. Thus, the heat flow is often written in the form

$$\frac{\mathrm{d}Q}{\mathrm{d}t} = mc_p\beta + f(T,t) \tag{1}$$

where m is the sample mass, c_p is the ''base-line'' specific heat capacity of the sample, which in general will be temperature dependent, β is the heating rate, and $f(T, t)$ represents the heat flow due to kinetic processes. The term ''base-line'' specific heat capacity here implies that it represents the heat capacity of a sample for which the structure remains constant. This terminology was introduced by Mathot [6], with particular reference to semi-crystalline polymers, to imply that no excess heat capacity occurs due to crystallisation or melting, and the idea is extended here to imply that no excess heat capacity arises from changes in the amorphous structure. In many cases, the constant structure will be that of equilibrium, thus defining for example the base-line heat capacities of a crystalline solid and of a liquid, respectively, before and after a melting process. In other cases, this may be a non-equilibrium structure but one which remains constant on the time scale of the measurement, thus defining, for example, the base-line heat capacity in

the non-equilibrium glassy state for an amorphous polymer below its glass transition temperature.

One of the most commonly used illustrations of the DSC heat flow signal is afforded by quenched polyethylene terephthalate (PET). This is because PET is a crystallisable polymer, but the crystallisation is inhibited by the quench, resulting in an amorphous material. On heating in the DSC, a glass transition is observed first, after which the material gains sufficient mobility for cold crystallisation to occur, which is then followed by the melting process. Thus, one can conveniently achieve a glass transition, crystallisation and melting in a single DSC heating scan, as shown in Fig. 1.

At the glass transition, there is an increase in specific heat capacity from that of the glass, c_{pg}, to that of the liquid, c_{pl}, in an approximately sigmoidal fashion, and hence an equivalent endothermic heat flow increase corresponding to the first term of Eq. (1), i.e. $mc_p\beta$. In fact, there is also a small endothermic peak visible within the glass transition interval in Fig. 1 resulting from the relaxation behaviour, and which reflects the contribution from the second term in Eq. (1), i.e. $f(T, t)$. It is not strictly correct, however, to separate these two components, as is implied by Eq. (1). While the base-line specific heat capacity, c_p, is uniquely defined in the glassy (c_{pg}) and liquid-like (c_{pl}) regions, where no structural changes are taking place, the definition of c_p in the transition region itself is *not* uniquely defined. Instead, it depends on the structural state in the transition region, which itself depends upon the path by which that state was reached, in other words on the thermal history of the sample. This is, of course, the origin of the endothermic peak, and is best illustrated with reference to the schematic enthalpy—temperature and specific heat capacity—temperature diagrams in Fig. 2a, where the endothermic peak is clearly seen in the heating scan for the heat capacity. As a consequence, in this transition region the heat capacity must be defined operationally rather than physically. The specific heat capacity is defined as the heat

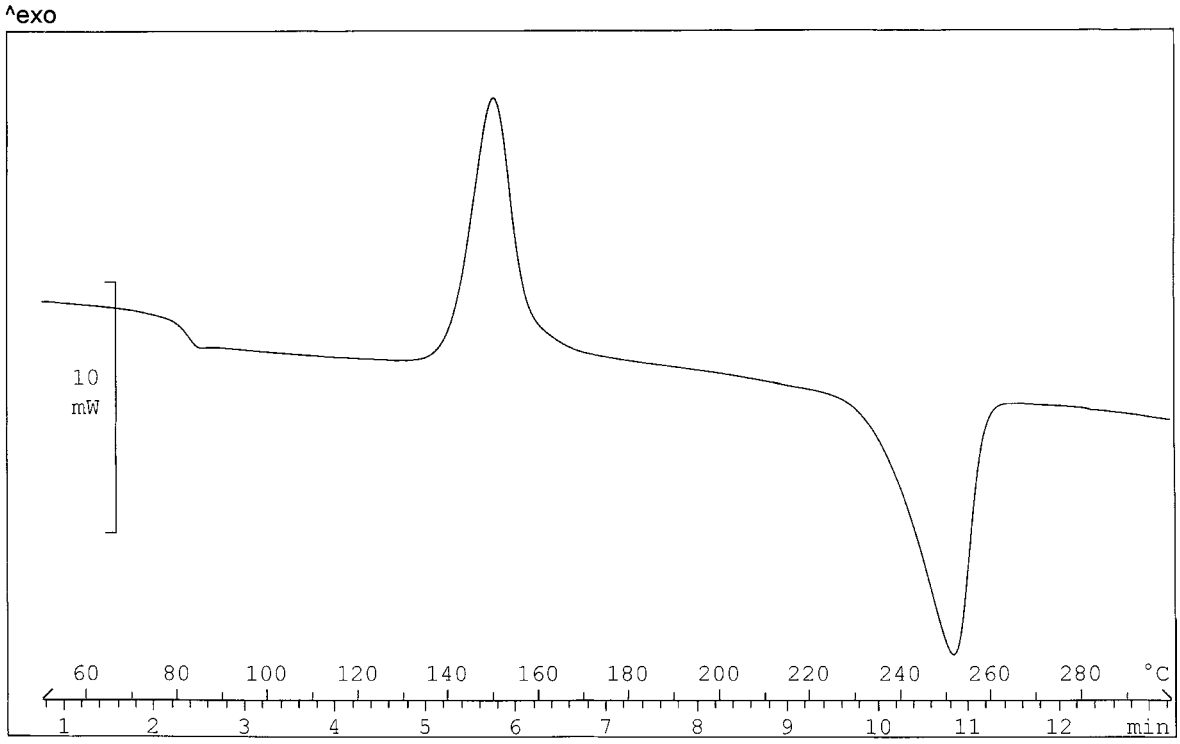

Fig. 1. DSC heating scan for polyethylene terephthalate quenched from 285 °C into liquid nitrogen, and then heated at 20 K min^{-1}. Sample mass = 11.70 mg.

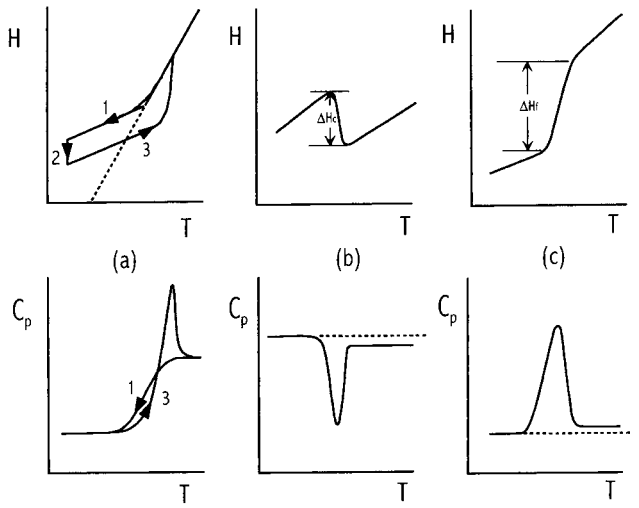

Fig. 2. Schematic enthalpy-temperature and specific heat capacity vs. temperature diagrams for: (a) the glass transition showing the cooling (1), isothermal annealing (2) and heating (3) stages of a thermal cycle; (b) the cold crystallisation process with enthalpy of crystallisation ΔH_c; and (c) the melting process, with enthalpy of fusion ΔH_f. (Remember that the heat capacity of a material is equal to the first derivative of its enthalpy with respect to temperature.)

required to raise the temperature of unit mass of a substance by one degree, so that the temperature rise ΔT for a heat input of Q is

$$\Delta T = \frac{Q}{mc} \tag{2}$$

where c is the specific heat capacity and m is the mass of the sample. At constant pressure, therefore, where the heat input is equal to the enthalpy change, the operational definition of the specific heat capacity becomes

$$c_p = \frac{1}{m}\frac{\mathrm{d}H}{\mathrm{d}T} = \frac{1}{m\beta}\frac{\mathrm{d}H}{\mathrm{d}t} \tag{3}$$

where H is the enthalpy of the sample. The quantity $\mathrm{d}H/\mathrm{d}t$ is just the heat flow in a quasi-equilibrium process at constant pressure, and hence we can see that the operational c_p defined by Eq. (3) is the sum of c_p and $(1/m\beta)f(T, t)$ in Eq. (1), that is the sum of the base-line and kinetic components. In other words, in the glass transition region it is not possible to separate the two heat flow components in Eq. (1), and there is no meaning to a base-line heat capacity when the structure is changing, as it is during the transition.

These arguments apply also to the crystallisation and melting processes. In the cold crystallisation process, there is a small decrease in the base-line heat capacity as a result of the crystallisation, which can be seen in Fig. 1 as a displacement in the exothermic direction of the base-line before and after the peak. Physically, this small decrease in c_p may be accounted for in terms of the loss of molecular mobility as the amorphous structure is ordered into a semi-crystalline arrangement. Within the crystallisation region, there is a substantial exothermic heat flow from the enthalpy of crystallisation, so the enthalpy-temperature diagram can be represented as in Fig. 2b. The base-line heat capacities before and after the transition are obviously easily defined, but within the transition region itself the situation is more complicated. Nevertheless, procedures have been proposed for the determination of the base-line in this region [6,7]. In view of there being only a small difference between the base-line heat capacities in the uncrystallised and crystallised states, it is tempting to consider c_p as a constant throughout and hence to separate the exothermic heat flow due to crystallisation as $f(T, t)$ in Eq. (1); it should be recognised, however, that this can be a misleading simplification, which is particularly well illustrated from a consideration of the melting process by TMDSC as will be shown later.

The melting process is similar to cold crystallisation in that there is a small difference between the base-line heat capacities before and after melting, as can be seen

in Fig. 1. Ideally, melting occurs at a single temperature, but such equilibrium conditions never occur in practice; furthermore, for polymers in particular there is usually a rather broad range of melting temperatures corresponding to the melting of crystallites of different degrees of perfection. Thus, the enthalpy of fusion is commonly spread over quite a wide temperature range, as illustrated in Fig. 2c. The effect is to cause the apparent heat capacity to pass through a broad peak on melting. Does this peak in c_p mean that the base-line heat capacity of the material is increasing and then decreasing during the melting process? The answer is surely "no", but it will be seen that TMDSC might appear to be interpreted in the opposite sense.

2.2. TMDSC

In TMDSC, a temperature modulation of amplitude A_T and frequency ω is superimposed on the underlying heating rate β. If the initial temperature is T_0, then the temperature at any time t is given by

$$T = T_0 + \beta t + A_T \sin \omega t \tag{4}$$

if we assume a sinusoidal modulation. The instantaneous heating rate is then given by

$$q = \frac{\mathrm{d}T}{\mathrm{d}t} = \beta + A_T \omega \cos \omega t \tag{5}$$

An illustration of some typical heating rate profiles is given in Fig. 3. Here, three different possibilities are shown: in Fig. 3a, each period includes both heating and cooling stages ("heat–cool"); in Fig. 3b, the sample is never cooled ("heat only"); in Fig. 3c, the cooling equivalent of Fig. 3b is shown ("cool only").

It is evident then that there is a periodic modulation of the heating rate between maximum and minimum values given by, respectively

$$q_{\max} = \beta + A_T \omega \tag{6}$$

$$q_{\min} = \beta - A_T \omega \tag{7}$$

By putting in some typical values for β, ω and A_T, we can immediately identify one of the professed advantages of TMDSC over DSC. Table 1 lists values of $q_{\max}$ and $q_{\min}$ for a number of typical modulation

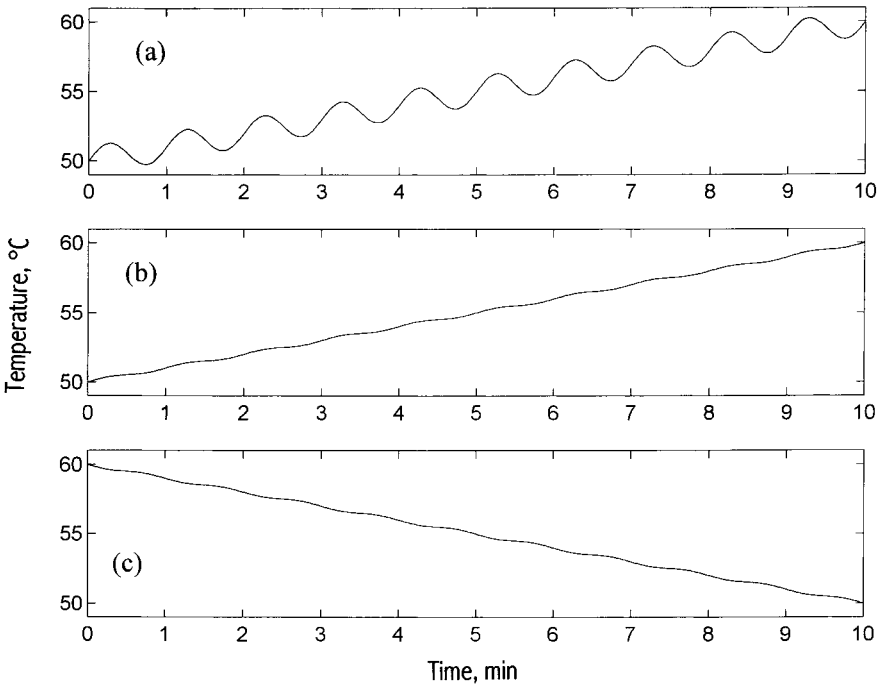

Fig. 3. Illustration of TMDSC temperature programmes: (a) $\beta = 1$ K min^{-1}, period = 1 min, $A_T = 1$ K, heat–cool cycles; (b) $\beta = 1$ K min^{-1}, period = 1 min, $A_T = 0.1$ K, heat only cycles; (c) $\beta = -1$ K min^{-1}, period = 1 min, $A_T = 0.1$ K, cool only cycles.

Table 1
Values of q_{max} and q_{min} from Eqs. (6) and (7), respectively, for typical values of the TMDSC parameters β, ω and A_T

β (K min^{-1})	Period (min)	ω (rad s^{-1})	A_T (K)	$A_T\omega$ (K s^{-1})	q_{max} (K min^{-1})	q_{min} (K min^{-1})
1	0.5	0.21	1	0.21	13.6	−11.6
	1	0.10	1	0.10	7.3	−5.3
	2	0.05	1	0.05	4.1	−2.1
1	0.5	0.21	0.5	0.10	7.3	−5.3
	0.5	0.21	1	0.21	13.6	−11.6
	0.5	0.21	2	0.42	26.1	−24.1
1	1	0.10	1	0.10	7.3	−5.3
2	1	0.10	1	0.10	8.3	−4.3
4	1	0.10	1	0.10	10.3	−2.3

conditions defined by β, ω (or period) and A_T. The underlying heating rate is considerably less than the typical value of 10 K min^{-1} used for DSC, for reasons that will become clear shortly. What can be seen from Table 1 is that instantaneous values of the heating (and cooling) rate similar to 10 K min^{-1} can be achieved with underlying heating rates much less than 10 K min^{-1}. For example, $\beta = 1$ K min^{-1} together with period = 1 min and $A_T = 1$ K, a combination abbreviated to (1, 1, 1) here for (β, per, A_T), gives $q_{max} = 7.3$ K min^{-1} and $q_{min} = -5.3$ K min^{-1}. As was mentioned earlier, the *sensitivity* of the calorimeter is increased with increasing heating rate, while the *resolution* improves with decreasing heating rate; hence in this example the TMDSC is able to combine the sensitivity of measurements at 7.3 and −5.3 K min^{-1} with the resolution of measurements at 1 K min^{-1}. Thus, in principle it is possible to traverse a thermal transition slowly whilst measuring the heat flow corresponding to instantaneously relatively large heating and cooling rates.

This appears at first sight to be a significant advance on the capabilities of conventional DSC. However, one must bear in mind certain assumptions that are inherently made. First, it is assumed that the average, for example, of heating at 7.3 K min^{-1} and cooling at −5.3 K min^{-1} will have exactly the same effect as heating at 1 K min^{-1}. This will be strictly true only if the response of the heat flow is linearly proportional to the heating rate and if the sample is able to follow the programmed heating/cooling rate. Taking each of these in turn, a linear response might be valid in temperature regimes distant from transitions, where no structural changes are taking place, such that the modulated heat flow is bounded by upper and lower limits of mc_pq_{max} and mc_pq_{min}, respectively; this is the approach involved in the "envelope analysis" offered as part of the Mettler Toledo software, and is illustrated in Fig. 4. Within a transition, however, where structural changes are occurring leading to complex time and temperature dependencies for the heat capacity, the assumption of a linear response is more difficult to justify. Under such circumstances, one could anticipate results which depend on the choice of experimental variables.

Second, the ability, or otherwise, of the sample to follow the heating rate modulations is also important. Just as for conventional DSC, there will be a thermal lag between the programmed temperature and the sample temperature as a result of heat transfer effects, and it would be quite likely, for example, that the sample could not follow the (1, 0.5, 2) modulations in Table 1, where instantaneous rates more than ±20 K min^{-1} appear. In conventional DSC, there are techniques, discussed earlier, which permit the calibration of the temperature scale to allow for such effects. In TMDSC, this is far from being so simple, and discussion of the effects of heat transfer has been presented in detail elsewhere (for example, see [8–17]).

Let us suppose, however, that we are satisfied that the response is linear and that heat transfer effects are either negligible or can somehow be allowed for. We wish now to progress to an analysis of the modulated heat flow signal that is the output from the TMDSC. Fig. 5 shows a typical result using (2, 1, 0.5) modulations, for the same quenched polyethylene terephthalate as was used for the conventional DSC results presented in Fig. 1, together with the heating rate modulations. The way in which these signals are analysed is by means of Fourier transformation.

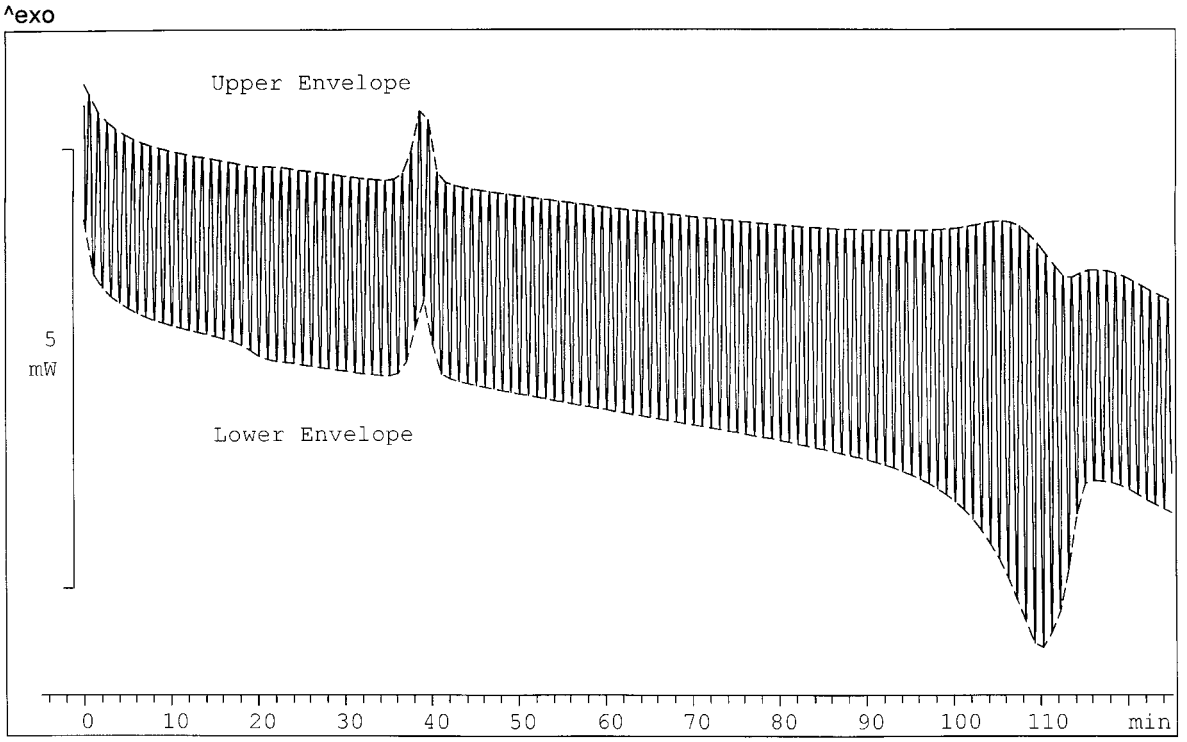

Fig. 4. Illustration of the "envelope analysis" applied to heating of a quenched PET sample, with underlying heating rate $\beta = 2\ \mathrm{K\ min^{-1}}$, period = 1 min, and amplitude $A_T = 0.5$ K.

All periodic functions can be expressed as the sum of sinusoidal components. Thus, any such periodic function can be represented by an infinite series of sinusoids with frequencies from the fundamental to the higher harmonics. The amplitudes of the various harmonic components of this series can be determined by routine mathematical procedures, but it often transpires that the amplitude decays rapidly with increasing frequency, so that in practice only the first few terms of the infinite series is adequate for a representation of the given periodic function.

An alternative approach is to utilise the Fourier transformation procedure, which transforms data from the time domain to the frequency domain, separating the time-dependent periodic function into components at different harmonic frequencies. An illustrative example may be useful to explain what this means. Rotating machinery such as motors, generators, turbines clearly involves periodic modulations, and at a constant frequency if the rotational speed is held constant. Thus, for example, the strain at the surface of a loaded rotating axle will vary in a sinusoidal way, and under normal circumstances this sinusoidal variation will continue as a function of time as long as the axle is rotating. The important aspect of this strain variation is not its time dependence, but the fact that its frequency remains constant, and hence the Fourier transformation to extract this frequency is useful.

Suppose now, though, that the bearings for this axle begin to wear, or some other fault occurs, introducing rough running. This will cause a complex variation in the stress and strain in the axle, such that the strain is no longer perfectly sinusoidal as a function of time. What the Fourier transformation does is to transform this time-dependent signal into the fundamental frequency component, corresponding to the basic rotation of the axle, together with other components at different frequencies corresponding to the contribution from the rough running arising from wear or misalignment of the bearings. The frequencies of

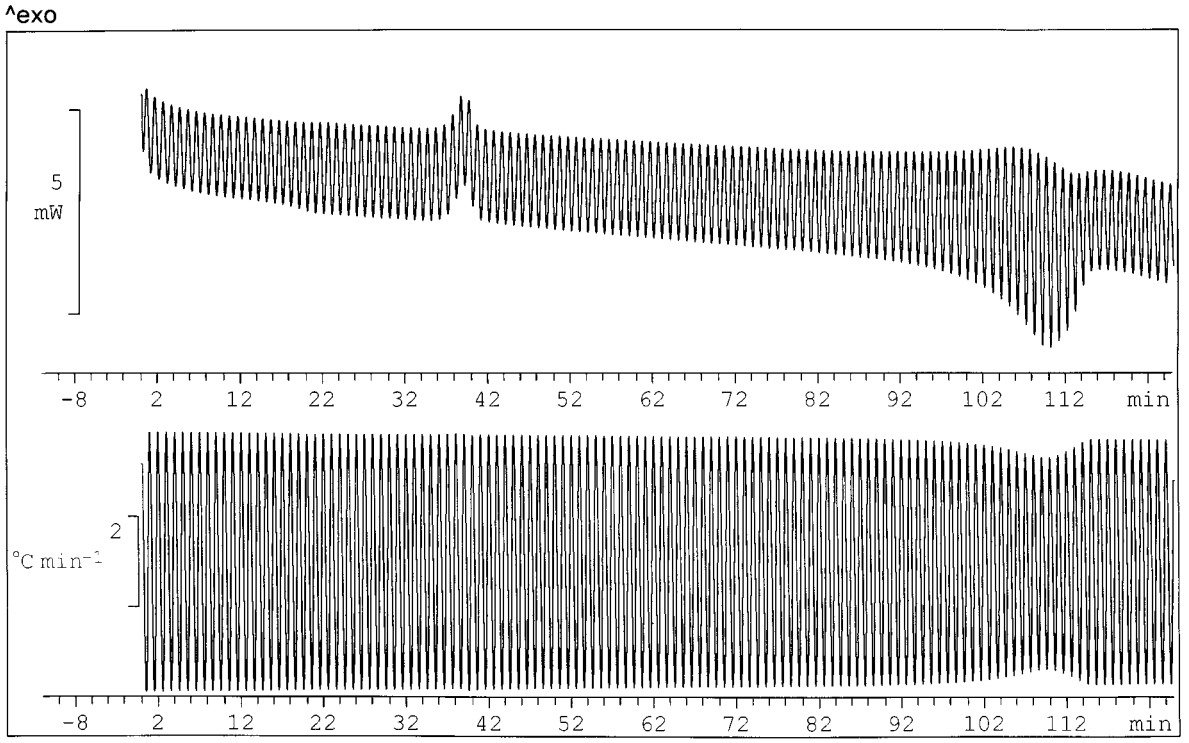

Fig. 5. Modulated heat flow for quenched polyethylene terephthalate with $\beta = 2$ K min^{-1}, period = 1min, and $A_T = 0.5$ K (upper); heating rate modulations (lower).

those other components can provide information about the nature of the fault in the bearing, while the magnitudes tell of its importance.

Thus, in Fig. 5, for example, since the heating rate modulation is purely sinusoidal (except in the melting region, to be discussed later) at the programmed frequency of 0.10 rad s^{-1} (period = 1 min), the Fourier transform will consist of only this single frequency. Likewise, in regions of the modulated heat flow curve distant from any transition, the sample will follow exactly the heating rate modulations if heat transfer to the sample is instantaneous, giving a Fourier transform of the heat flow curve consisting of the same single frequency as for the heating rate modulations. It will also have the same phase as the heating rate modulations, but with an amplitude dependent on the heat capacity of the sample. If, however, heat transfer to the sample were not instantaneous (as, of course, would be the situation in practice), then the heat flow modulations would have the same frequency as the heating rate modulations, but displaced by a phase angle (equivalent to a time lag in the time domain).

On the other hand, in regions where the sample is undergoing a transition, in which there are additional kinetic heat flow contributions due to endothermic or exothermic processes (analogous to the contributions from rough running of the bearings discussed above), the heat flow modulations will now contain components at frequencies other than the fundamental frequency of the heating rate modulations. The usual practice in TMDSC is to consider only the contribution from the fundamental frequency, though it is possible with the Mettler Toledo software to access the higher harmonics. In general, there will in addition be a phase change also, and an amplitude dependent on the nature of the transition, as will be discussed further below.

Before considering the way in which the analysis of the modulated heat flow and heating rate signals is implemented in TMDSC, it is useful to examine the heat flow modulations in a more quantitative way. The

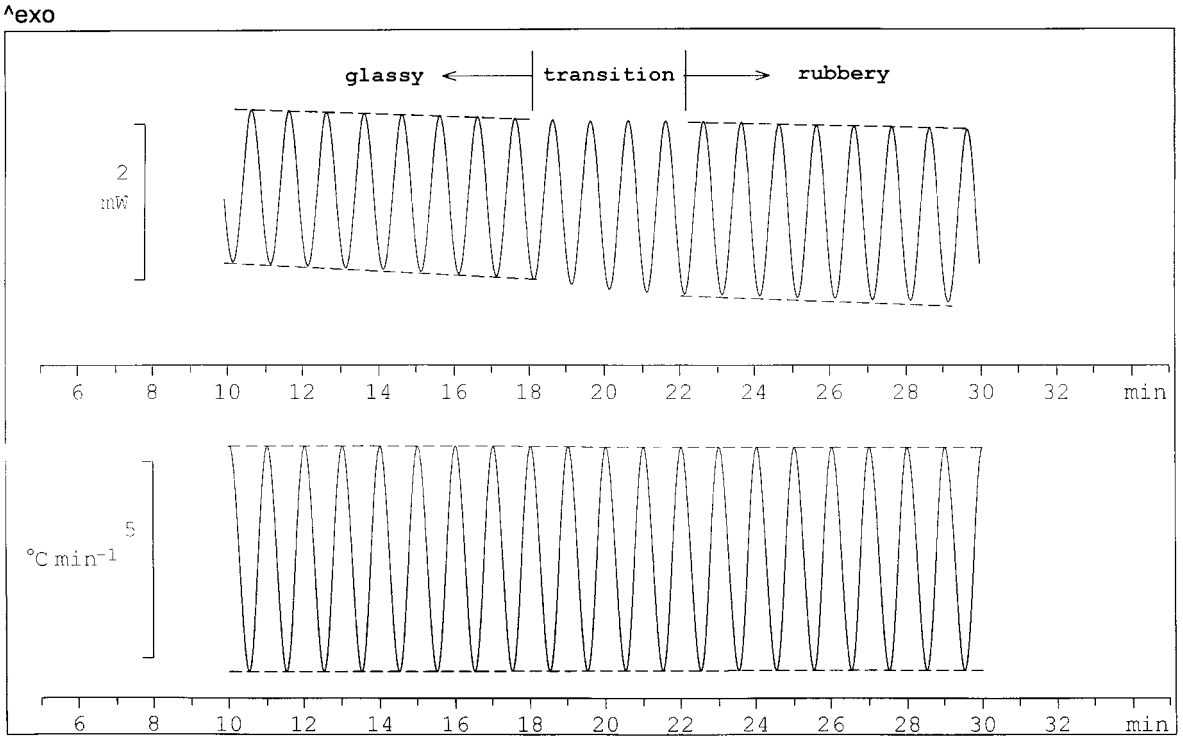

Fig. 6. Heat flow and heating rate modulations for the glass transition region of quenched PET (expanded region from Fig. 5). The dashed lines are drawn to indicate the regions of constant amplitude of either heat flow or heating rate.

example of TMDSC applied to quenched PET in Fig. 5 provides an excellent illustration for these purposes. Consider first the glass transition, shown expanded in Fig. 6, where only the modulated signal is considered.

Here it can be seen that the amplitude of the heat flow modulations in the glassy region is constant, and in the rubbery or liquid-like region above the glass transition the amplitude is again constant, but somewhat greater than that in the glassy region. Between these two regions, in the transition interval itself, there appears to be a rather uniform increase in amplitude of the modulations. These observations can be rationalised as follows. The heat flow modulations arise from the base-line heat capacity of the sample together with the imposed temperature changes or heating rates. In the glassy state, the only contribution to the heat capacity, within the timescale of the modulation period, comes from vibrational motions with relaxation times of the order of 10^{-13} s. In the liquid-like state above the glass transition, there are contributions to the heat capacity from both vibrational and segmental motions. The latter have timescales of the order of 100 s at T_g, and this timescale will decrease as the temperature increases, in a manner dependent upon the activation energy. Below T_g the timescale of these segmental motions is many orders of magnitude larger. Hence, at some temperature above the transition, the time scale of these segmental motions will have decreased below that of the modulations. Within the transition interval, though, as the temperature increases there will be a gradual change from glassy to liquid-like response as the timescale for the segmental motions decreases thus providing a gradual increase in their contribution to the heat capacity, and hence to the heat flow.

The exact course of this gradual change will depend upon the actual magnitudes of the timescales for these segmental motions, which are determined by the instantaneous structure of the glassy material. As long as the underlying heating or cooling rate is sufficiently small, then the structural state (or enthalpy) of the sample will be insignificantly different between start

and finish of any one period, and therefore there will be no significant contribution to the modulated heat flow from irreversible structural (i.e. enthalpic) changes during the modulations [18]. This implies that only the reversible heat flow necessary to change the temperature of the sample will contribute to the heat flow amplitude in the glass transition region. This will not always be the case, however. In particular, glasses that have been well annealed before scanning in TMDSC can show a very rapid change in enthalpy with time such that irreversible changes could occur within one period.

In the cold crystallisation transition in Fig. 5, shown expanded in Fig. 7, there again appears to be rather little change in the amplitude of the heat flow modulations. One might anticipate a small reduction in the amplitude as a result of the change from an amorphous structure to a crystalline (or semi-crystalline) structure, since the heat capacity of the crystalline phase is less than that of the amorphous phase. Indeed, there is evidence for a reduction in the average value of heat capacity before and after the cold crystallisation process when one examines the average heat flow curve in Fig. 7. Such a small change in the heat flow amplitude would not be evident simply from an examination of the modulations in Fig. 7, but would require the more detailed analysis, to be described below, to make it discernible. In addition to such effects, though, in this cold crystallisation region there is the opportunity, during any one modulation period, for there to occur a certain amount of crystallisation. For example, there are some nine periods within the cold crystallisation range (Fig. 7), and if the crystallinity of PET at the end of cold crystallisation were 20%, say, then each period would involve a change of about 2% in the crystallinity. If this represented a significant difference between the crystallinity at the beginning and end of any period, then it would contribute to the observed amplitude of heat flow during that cycle, the major part of which results from the base-line heat capacity of the sample. Evidently, the timescale for cold crystallisation in PET is sufficiently slow for there to be no

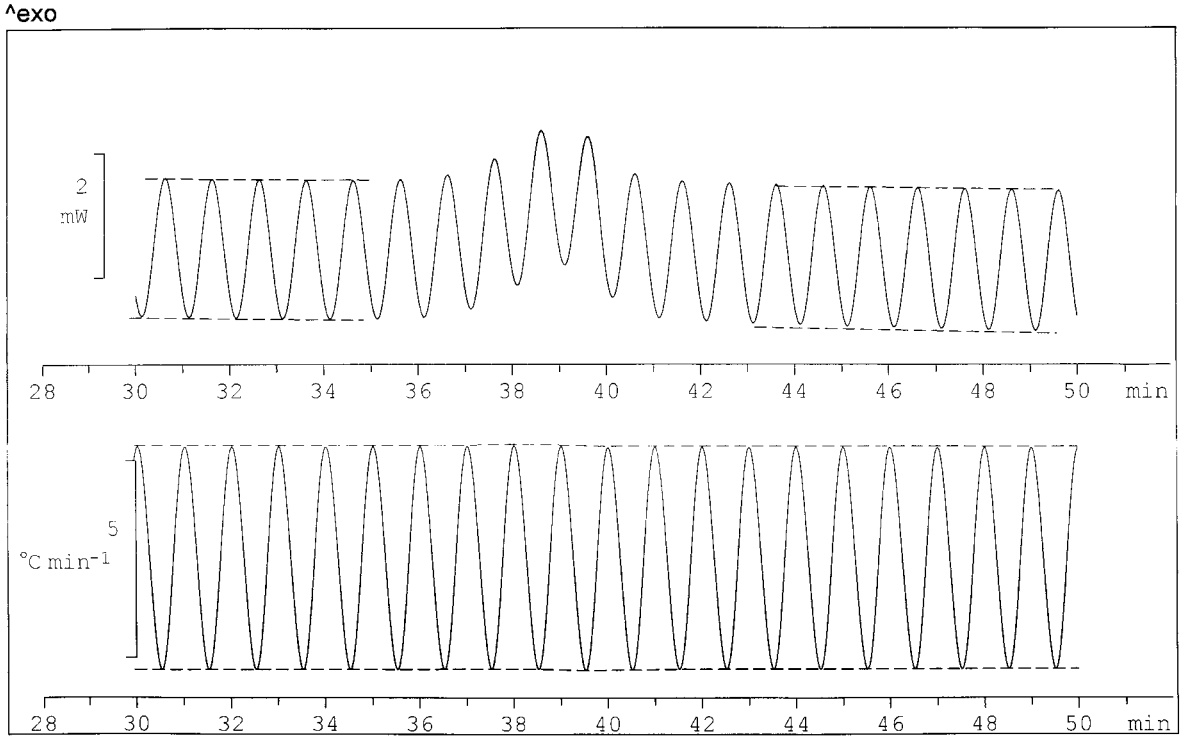

Fig. 7. Heat flow and heating rate modulations for the cold crystallisation region of quenched PET (expanded region from Fig. 5). The dashed lines are drawn to indicate the regions of constant amplitude of either heat flow or heating rate.

immediately noticeable effect on the heat flow modulation. Alternatively, the apparently constant amplitude of heat flow during the cold crystallisation process may imply that the rate of crystallisation is insensitive to the instantaneous heating rate. It will be seen later, however, that when the heat flow amplitude is examined in detail in this region, it is possible to identify the effect of this contribution from crystallisation during a single cycle.

Turning now to the heat flow modulations seen during the melting region of PET in Fig. 5, shown expanded in Fig. 8, it is clear that a quite different situation prevails. Here there is a marked increase in the amplitude of the heat flow modulations during the course of the melting process, before it returns to a constant amplitude, similar in magnitude to that before the start of melting. In fact, there is again good reason to believe that the amplitude before melting will be slightly less than that after melting since the heat capacity is expected to be higher in the melt phase than in the solid crystalline phase. It is interesting to consider why the heat flow amplitude should show such a marked increase during melting, and in doing so it is obviously relevant to make comparison with the cold crystallisation behaviour. Just as it was possible for a certain amount of crystallisation to occur during any one modulation period within the cold crystallisation peak, here it is possible for a certain amount of melting to occur during a single cycle. But there are two important distinctions to be made between the melting and cold crystallisation process in TMDSC: the first concerns the relative timescales for each process and the second concerns the possibility of both melting and crystallisation occurring in the same cycle.

Considering first the relative timescales, it is clear that the process of melting will occur more rapidly than cold crystallisation since the temperature is significantly higher for the melting regime. Hence, whereas the ideal requirement that the structure be the same at the start and finish of a single modulation period could be met approximately for cold crystallisation, this is likely to be rather harder to meet in the

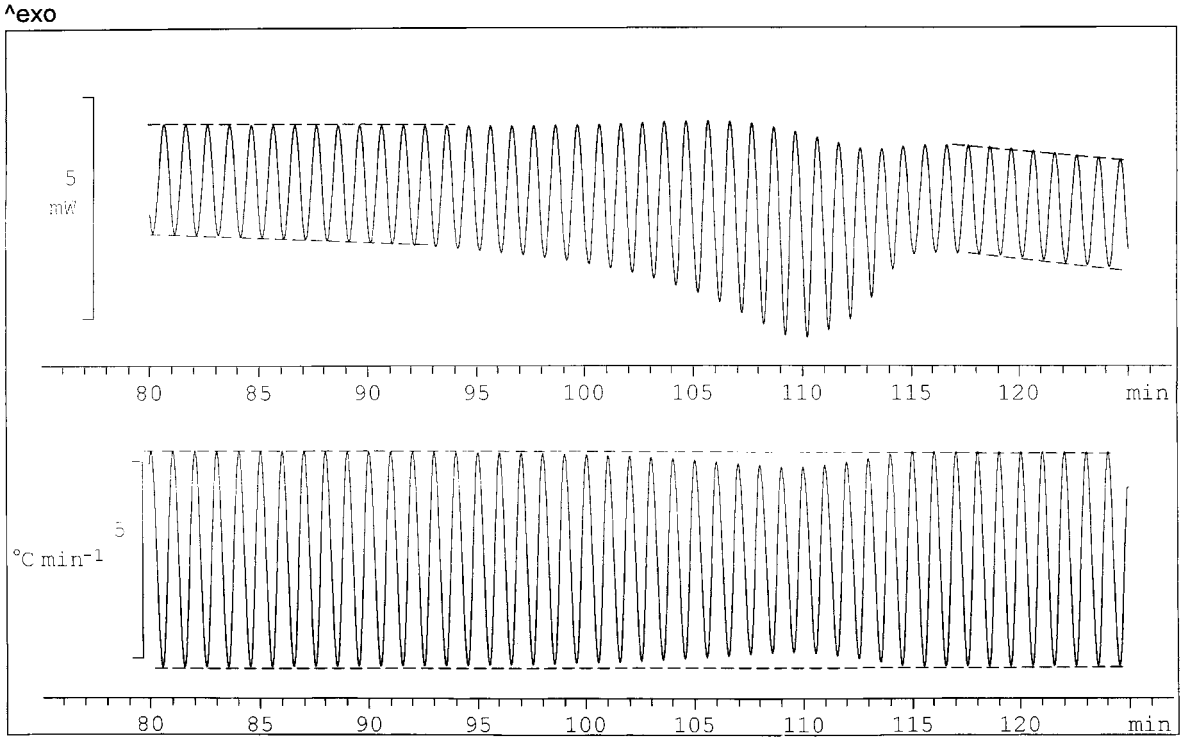

Fig. 8. Heat flow and heating rate modulations for the melting region of quenched PET (expanded region from Fig. 5). The dashed lines are drawn to indicate the regions of constant amplitude of either heat flow or heating rate.

case of melting. This problem is further compounded by the second distinction mentioned above, namely that both melting and crystallisation may be possible in a single cycle. This can be quite a complex situation, particularly for polymers which are known to exhibit in general a rather broad melting region compared with a much narrower interval for the melting of pure metals, for example. Furthermore, the degree of crystal perfection can increase on annealing at temperatures close to the equilibrium melting temperature, so that a process similar to crystallisation may occur during even very small amplitude modulations.

Additionally, if the amplitude is sufficiently large in combination with given values of frequency of modulation and underlying heating rate, it is possible for the heating rate modulations to include both heating and cooling stages in a single cycle. For example, the modulation conditions used for PET in Fig. 5, the (2, 1, 0.5) cycle, has maximum and minimum heating rates of 5.1 and -1.1 K min^{-1}, respectively, which is clearly a ''heat–cool'' cycle. In order to ensure a ''heat only'' cycle, the temperature amplitude of the modulations in Fig. 5 would have to be reduced to 0.32 K, an approximately 36% reduction that would give rise to 36% reduction in the heat flow amplitude associated with the base-line heat capacity, and hence having some disadvantageous effects in respect of sensitivity. On the basis of the above reasoning, therefore, it is possible to rationalise the variation of the amplitude of the heat flow modulations during melting. As melting proceeds, in any one cycle there will be a rise in temperature causing further melting to occur, accompanied by both the heat flow necessary to raise the temperature and the latent heat of fusion, followed by a fall in temperature allowing some recrystallisation to occur, itself accompanied by the heat flow associated with the temperature reduction as well as any heat of crystallisation. The heat of fusion and crystallisation will thus contribute to the amplitude of the heat flow modulation, appearing as if they are reversible heat flows. In fact, these are not really reversible heat flows since they are accompanied by structural changes in which the degree of crystalline order is different between the beginning and the end of the cycle. Although the above rationalisation is given in respect of a ''heat–cool'' cycle such as was used to obtain the curves in Fig. 8, similar arguments would also apply to a ''heat only'' cycle. In this case, melting would be occurring continuously, but at a variable rate of endothermic heat flow, while crystalline reordering rather than recrystallisation would simultaneously contribute an exothermic component to the modulated heat flow.

A common feature of the heat flow response, and of the heat flow modulations in particular, is that the sample is not in thermodynamic equilibrium in any of the transitions discussed with respect to Fig. 5. At the glass transition, the amplitude of the modulations depends upon whether the sample exhibits a non-equilibrium glassy response or an equilibrium liquid-like response. In the cold crystallisation region, the amorphous structure is clearly energetically a long way from an equilibrium crystalline state, but a quasi-isostructural condition applies to each modulation cycle by virtue of the timescale for structural changes being sufficiently long in comparison with the period. In contrast, the melting process, which will always be non-equilibrium except at infinitesimally slow heating rates, allows structural rearrangements such as melting, recrystallisation and reordering to occur on timescales that are not long compared with the modulation period, and which can therefore contribute to the modulated heat flow.

In general, therefore, we cannot write the enthalpy H as a function of temperature T and pressure P, alone, as would be the case for classical equilibrium thermodynamics. Instead, we must include the dependence of H on some order parameter ξ

$$H = H(T, P, \xi) \tag{8}$$

where the definition of the order parameter will be specific to the particular transition involved. For example, in the glass transition region it may be the excess enthalpy, while for crystallisation and melting it may be the degree of crystallinity.

At constant pressure, the enthalpy is a function only of T and ξ, and its total differential may therefore be written as

$$\mathrm{d}H = \left(\frac{\partial H}{\partial T}\right)_{\xi} \mathrm{d}T + \left(\frac{\partial H}{\partial \xi}\right)_{T} \mathrm{d}\xi \tag{9}$$

and hence one can derive the differential of H with respect to T

$$\frac{\mathrm{d}H}{\mathrm{d}T} = \left(\frac{\partial H}{\partial T}\right)_{\xi} + \left(\frac{\partial H}{\partial \xi}\right)_{T} \frac{\mathrm{d}\xi}{\mathrm{d}T} \tag{10}$$

Note that the use of the subscripts ξ and T implies constant structure and temperature, respectively. The left-hand side of this equation is simply the apparent heat capacity (see Eq. (3)), whereas the first term on the right hand side is the thermodynamic or base-line heat capacity. The equality of the apparent or measured heat capacity with the base-line heat capacity therefore relies upon the second term on the right hand side being zero. This will occur under conditions in which the structural state of the sample, identified by the order parameter, remains constant. Hence, we can understand the importance of the relative timescales for the molecular motions and for the temperature modulations, since we require that ξ changes only insignificantly during a single period. This is essential for the interpretation of the amplitude of the modulated heat flow in terms of a base-line heat capacity.

If we turn now to heat flows by multiplying Eq. (10) throughout by a constant heating rate $\mathrm{d}T/\mathrm{d}t$, we get

$$\frac{\mathrm{d}H}{\mathrm{d}t} = mc_{pb}\frac{\mathrm{d}T}{\mathrm{d}t} + \left(\frac{\partial H}{\partial \xi}\right)_T \frac{\mathrm{d}\xi}{\mathrm{d}t} \tag{11}$$

where the subscript 'b' for the specific heat capacity refers to its base-line value, and hence the DSC signal P is given by

$$P_{\mathrm{DSC}} = mc_{pb}\beta + \left(\frac{\partial H}{\partial \xi}\right)_T \frac{\mathrm{d}\xi}{\mathrm{d}t} \tag{12}$$

where β is the heating rate. The term $\mathrm{d}\xi/\mathrm{d}t$ has been written thus rather than as the equivalent $\beta\mathrm{d}\xi/\mathrm{d}T$ in order to emphasise that it represents the time rate of change of the order parameter, which is determined by the kinetics of the process involved, whether it be a glass transition, a crystallisation or a melting process. In general, the time rate of change of the order parameter will depend upon both the degree of order itself and the temperature, the latter typically through an Arrhenius dependence, such that

$$\frac{\mathrm{d}\xi}{\mathrm{d}t} = f(\xi)\exp\left(-\frac{E}{RT}\right) \tag{13}$$

where E represent the activation energy for the process. Thus, the apparent heat capacity, evaluated as the DSC power output divided by the heating rate, will be time (and temperature) dependent, as already represented by the time and temperature dependent heat flow term $f(T, t)$ in Eq. (1)

$$\frac{P_{\mathrm{DSC}}}{\beta} = mc_{pb} + \left(\frac{\partial H}{\partial \xi}\right)_T \frac{\mathrm{d}\xi}{\mathrm{d}T} \tag{14}$$

On the other hand, if the heating rate $\mathrm{d}T/\mathrm{d}t$ in Eq. (11) (remembering that $\mathrm{d}\xi/\mathrm{d}t = \beta(\mathrm{d}\xi/\mathrm{d}T)$) is now given by Eq. (5) as the sum of an underlying heating rate β and a periodically modulated component $A_T\omega\cos\omega t$, then the TMDSC power P is given by

$$P_{\mathrm{TMDSC}} = mc_{pb}[\beta + A_T\omega\cos\omega t] + \left(\frac{\partial H}{\partial \xi}\right)_T \frac{\mathrm{d}\xi}{\mathrm{d}T}[\beta + A_T\omega\cos\omega t] \tag{15}$$

which can be written from Eq. (14) as

$$P_{\mathrm{TMDSC}} = P_{\mathrm{DSC}} + \left[mc_{pb} + \left(\frac{\partial H}{\partial \xi}\right)_T \frac{\mathrm{d}\xi}{\mathrm{d}T}\right] A_T\omega\cos\omega t \tag{16}$$

From this we can identify two components contributing to the TMDSC power. The first is the same as the DSC power, and is an underlying heat flow which, as has been shown, is dependent on the underlying heating rate; this gives rise to a heat capacity that is, in general, time and temperature dependent.

The second component is the modulated heat flow. In general, this is complicated by the second term within square brackets, which represents the contribution to the heat capacity from structural changes and associated enthalpy changes occurring during a modulation period. In order to evaluate this contribution, it is necessary to know the detailed kinetics of the time and temperature dependence of these structural changes, such as is given by Eq. (13) for example. It is common to assume, for simplicity, that this second term within square brackets in Eq. (16) is negligible, but this assumption should be considered with extreme caution. In particular, it is a very poor assumption, and can indeed be misleading, when applied to melting and to the glass transition of annealed glasses, for both of which there are significant structural changes occurring during any one period.

However, if we assume for the present that we may neglect this term, then the amplitude of the second, modulated, component to the TMDSC heat flow can be written simply as

$$A_{\mathrm{HF}} = mc_{pb}A_T\omega \tag{17}$$

Since the amplitude of the heating rate modulations from Eq. (5) is

$$A_q = A_T\omega \tag{18}$$

we can define an apparent specific heat capacity from these heat flow modulations as

$$c_{p\mathrm{b}} = \frac{A_{\mathrm{HF}}}{mA_q} = c_{p\mathrm{b}} \tag{19}$$

This may be referred to as the reversing heat capacity, ($c_{p,\mathrm{rev}}$) for reasons that will become clear shortly, and is different from the heat capacity defined by Eq. (14) for DSC in one important respect. Whereas the latter is temperature (and time and heating rate) dependent, $c_{p,\mathrm{rev}}$ is frequency dependent. Thus, $c_{p\mathrm{b}}$ in Eq. (19) represents the instantaneous heat capacity as measured by temperature or heating rate modulations with a certain frequency (or period). Thus, for example, in the glass transition region the observed $c_{p,\mathrm{rev}}$ will depend upon whether or not the modulation period permits the contribution of molecular segmental motions; if not, then $c_{p,\mathrm{rev}}$ will measure a glassy heat capacity, whereas if yes, then $c_{p,\mathrm{rev}}$ will measure a liquid-like heat capacity. Hence, $c_{p\mathrm{b}}$ in Eq. (19) is different from that in Eq. (14), which depends on time (rather than frequency) in the sense that the measured value will depend again upon whether or not the sample has time for the segmental motions to contribute to the heat capacity, which will be determined of course by the heating rate.

The attractiveness of neglecting the ''offending'' term in Eq. (16) is obvious if we further ignore the important distinction between $c_{p\mathrm{b}}$ in Eqs. (14) and (19). These two ''simplifications'' together mean first that $c_{p\mathrm{b}}$ can be evaluated from Eq. (19). The underlying heat flow in Eq. (16), sometimes referred to as the *total* heat flow $\mathrm{HF_{tot}}$ (for reasons that will become clear shortly), is now noted as being the same as P_{DSC}, which is given by Eq. (12) as the sum of a term depending on $c_{p\mathrm{b}}$ and a ''kinetic'' heat flow term. The first of these is simply the product of $c_{p\mathrm{b}}$ (or $c_{p,\mathrm{rev}}$), found from Eq. (19), and the underlying heating rate, and is referred to as the *reversing heat* flow, $\mathrm{HF_{rev}}$, hence the use of the term ''reversing'' for the heat capacity in Eq. (19). This obviously leaves the second term in Eq. (12) as the difference between the total heat flow and the reversing heat flow, and is (seemingly logically) called the *non-reversing* heat flow, $\mathrm{HF_{non\text{-}rev}}$

$$\mathrm{HF_{non\text{-}rev}} = \mathrm{HF_{tot}} - \mathrm{HF_{rev}} \tag{20}$$

This would appear to be quite an appealing analysis, but it is worth reiterating the assumptions that have been made in its development: (i) that there is no contribution to the modulated heat flow from structural changes occurring during a cycle; and (ii) that the frequency dependent base-line heat capacity is the same as that found from DSC, and which is dependent on the timescale of the underlying heating rate.

The first of these assumptions is valid when the sample is distant from any transition, in other words when it is in an equilibrium or isostructural state. Under these conditions, the base-line heat capacity is indeed the same from both the modulations and the underlying heating rate, in other words the second assumption is also valid, so that $\mathrm{HF_{tot}}$ is then identical to $\mathrm{HF_{rev}}$, and there is no non-reversing heat flow. Whilst this situation renders the assumptions valid, however, the result is entirely unremarkable: all that it tells us is that outside a transition region the modulated heating rate gives rise to a reversible modulated heat flow.

On the other hand, within a transition region neither of these assumptions is strictly valid, and the question is whether or not either or both remain good approximations. There is no simple answer to this, and it is probably true to say that their validity or otherwise is determined after the event. Thus far, it appears that they remain reasonable approximations for glass transitions of unannealed glasses and cold crystallisation, but not for melting or for annealed glasses, at least in polymers.

It is evident, therefore, that the reversing and non-reversing heat flow approach leaves something to be desired, and as a consequence the interpretation of these supposed heat flow contributions to any given transition must be made with some care. There is, however, an alternative approach to the analysis of the TMDSC heat flow given by Eq. (16). This is to define a *complex* specific heat capacity c_p^* as the ratio of the amplitude of specific heat flow and heating rate, similar to Eq. (19)

$$c_p^* = \frac{A_{\mathrm{HF}}}{mA_q} \tag{21}$$

but to recognise that the contribution of the structural changes during any one period will have the effect of changing both the amplitude and the phase of the heat flow modulations. Thus, c_p^* is complex in the sense that it has two components, one in phase with the heating rate modulations (c_p') and the other out-of-phase (c_p''), defined as

$$c_p' = c_p^* \cos\phi \tag{22}$$

$$c_p'' = c_p^* \sin\phi \tag{23}$$

where ϕ is the phase angle.

This would appear to be a more logical approach than separating the total heat flow into reversing and non-reversing components. Here we have an underlying heat flow, from which an apparent heat capacity can be obtained, and a modulated heat flow, from which a frequency dependent complex heat capacity can be obtained, with components in-phase and out-of-phase with respect to the heating rate and determined by a phase angle ϕ. The in-phase component may be considered as the thermodynamic heat capacity, (c_p' at zero frequency) since it is directly related to the heat flow that is in phase with the heating rate.

The problem with this approach is that, at present, there is no universally acknowledged interpretation of the meaning of the out-of-phase component c_p'' (e.g. see [19–22]). If the phase angle is small, the in-phase component c_p' is very nearly equal to c_p^* and hence very nearly equal also to the reversing heat capacity $c_{p,\mathrm{rev}}$. On the other hand c_p'' should not be approximated to a non-reversing heat capacity. This problem is more of fundamental interest than of practical interest since, as is shown elsewhere [12,15–17], the measurement of the phase angle experimentally is severely complicated by another problem, that of heat transfer, which introduces an additional "instrumental" phase angle. Thus, the accurate experimental evaluation of the phase angle is an issue that is still unresolved for most transitions, indeed for any other than the glass transition, and hence it is not possible to investigate experimentally the out-of-phase heat capacity for different materials and different transitions. This must be an avenue to pursue in the future.

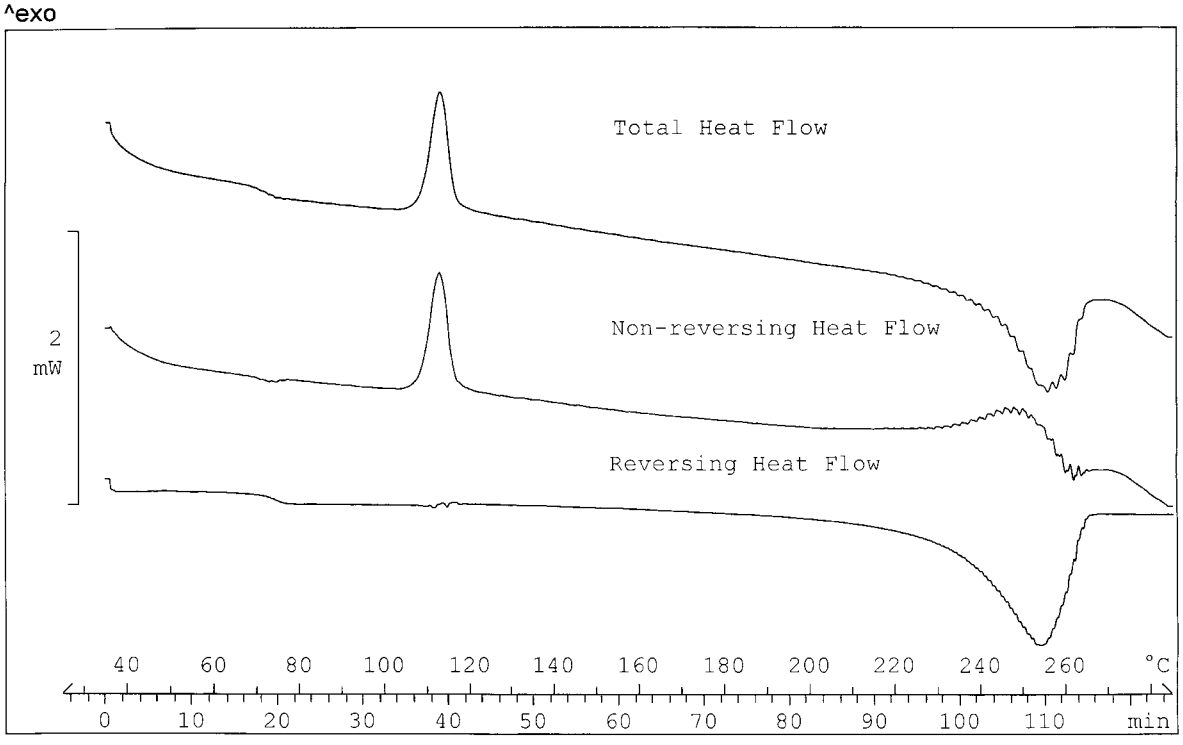

Fig. 9. Total, reversing and non-reversing heat flows derived from the modulated signals for polyethylene terephthalate in Fig. 5.

It should be emphasised here that the two approaches discussed here, namely reversing/non-reversing and complex heat capacity, are not mutually exclusive: any one set of TMDSC data may be analysed and interpreted using either or both of these approaches. In doing so, though, the limitations inherent in each approach in the light of the discussion above must be borne in mind if a realistic and meaningful interpretation of the data is to be achieved. To overlook such limitations is likely to lead to confusion.

2.3. Fourier transformation

Whether the analysis be done in terms of reversing and non-reversing heat flows, or in terms of a complex heat capacity, the modulated signals for heat flow and heating rate must be transformed into average values and amplitudes, and additionally to give a phase angle for the complex heat capacity representation. The way that this is done is the same for all the commercial instruments, and involves a "window" of one modulation period of the heating rate which is slid along the time scale of the heating (or cooling) scan. For each position of this sliding window, a Fourier Transform is applied to the heat flow signal in order to extract an average value $\langle \mathrm{HF} \rangle$, an amplitude A_{HF} and a phase angle ϕ, and these are compared with transformed variables from the sliding window of the heating rate modulations, namely the average heating rate $\langle q \rangle$ and the heating rate amplitude A_q.

The average heat flow thus obtained is also called the total heat flow, $\mathrm{HF_{tot}}$. The reversing heat flow $\mathrm{HF_{rev}}$ is $\beta A_{\mathrm{HF}}/A_q$ and the non-reversing heat flow is simply $\mathrm{HF_{tot}} - \mathrm{HF_{rev}}$, as given by Eq. (20). The result of this transformation for the modulated signals given earlier in Fig. 5 is shown in Fig. 9.

Alternatively, we may find the complex heat capacity from Eq. (21) and separate it into its two components, c_p' and c_p'', using the phase angle. The complex, in-phase and out-of-phase specific heat capacities are shown in Fig. 10, together with the variation of the phase angle, for the same modulated signals for polyethylene terephthalate given earlier in Fig. 5.

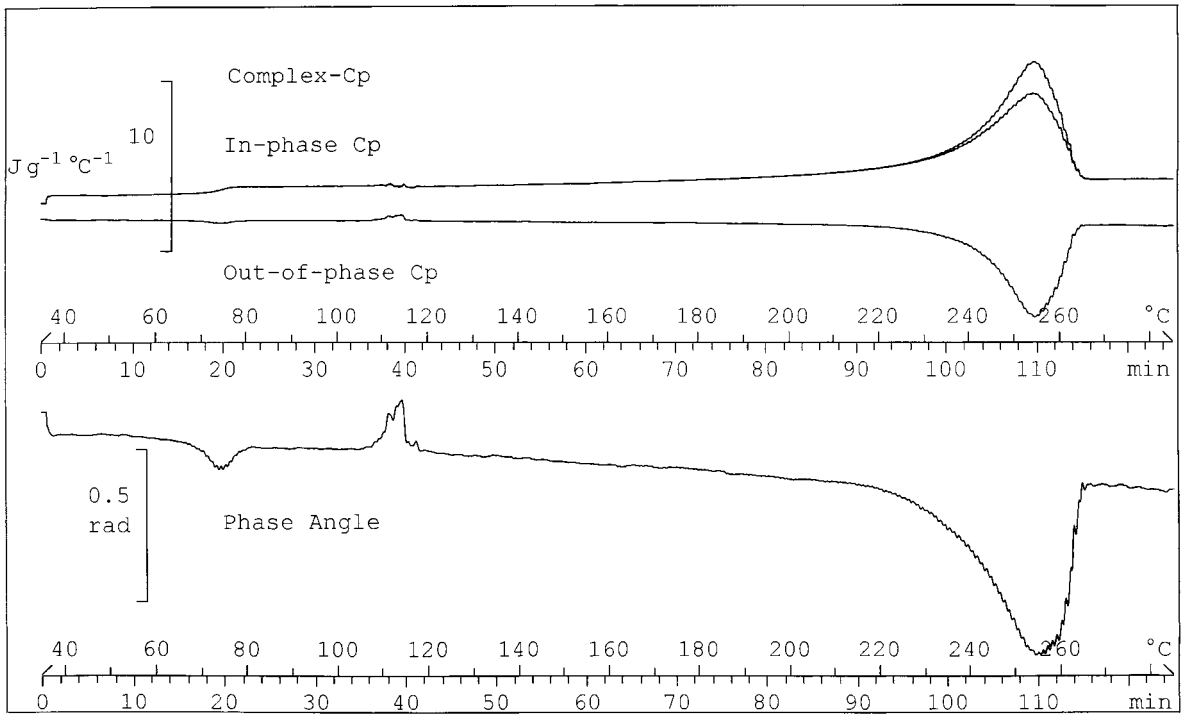

Fig. 10. Complex specific heat capacity, c_p^*, in-phase specific heat capacity, c_p', out-of-phase specific heat capacity, c_p'', and phase angle, ϕ, derived from the modulated heat flow and heating rate curves for polyethylene terephthalate in Fig. 5.

There is clearly a lot of information available from the numerous traces in Figs. 9 and 10, only two of which are equivalent (HF_{rev} and c_p^*). Furthermore, different information is available from each trace in the different transition regions. The interpretation of these curves will be dealt with elsewhere, but there are some general aspects which are worth some preliminary consideration.

First, it is evident that the traces in Figs. 9 and 10 are not smooth; there is a kind of ripple superimposed on the heat flow, heat capacity and phase angle curves, and it is particularly evident in the transition regions. The origin of these ripples lies in the windowing procedure for the Fourier transformation, whereby a window of exactly one cycle of the heating rate modulations is successively applied to and slid along the heat flow modulations [23]. Any departure of the heat flow modulation average value from a level base-line will mean that the start and end points of this window will be different, which will have an effect on the amplitude and average value of the transformed signal. This effect will be periodic as the window start (and end) point follows the periodic modulations of the heat flow, thus creating the ripples.

Second, since the amplitude of the heat flow modulations, derived from the Fourier transformation procedure, is used in the evaluation of the reversing heat capacity (Eq. (19)) and complex heat capacity (Eq. (21)), the departure of the average heat flow from a level base-line will have an unwanted influence on both of these heat capacities. This will render it difficult to interpret qualitatively the reversing or complex heat capacity within transition regions, and particularly in those regions where the average heat flow displays a strong variation, such as a rapid step change or a large peak. In order to overcome this problem, the Fourier transformation procedure is performed twice. The first transformation yields, amongst other things, the average heat flow, which will show all of the relevant transitions as in conventional DSC. This average heat flow trace is then subtracted from the original modulated heat flow, to give a modified heat flow signal which contains the modulations without the deviations in the average value. The second Fourier transformation procedure is now performed on this modified heat flow signal, which will yield the required amplitude A_{HF} to be used in the evaluation of the reversing heat flow and complex heat capacity.

3. Concluding remarks

The question of whether the reversing and non-reversing heat flow approach or the complex heat capacity approach is the better will no doubt continue to be debated for some time yet. The former is the more widely used, probably as a result of its being inherent to modulated DSC (MDSC), the technique originally patented by TA Instruments and still the market leader. However, its validity has been called into question here by making reference to basic principles, and it is suggested that the complex heat capacity has a more logical foundation. Nevertheless, the complex heat capacity itself has some disadvantages, most notably the present lack of a useful interpretation of its out-of-phase component. Attempts to make some deductions about its interpretation by means of experimental observations are hampered by the problem of heat transfer, which can have a significant influence on the value of the phase angle and hence on the out-of-phase heat capacity.

In addition, the interpretation of any TMDSC data relies heavily on the need to incorporate sufficient modulations within any transition such that each modulation remains *quasi*-isostructural. Often this will involve a reduction in the period to such an extent that the heat transfer problem then becomes significant. Thus, the choice of parameter values (β, per, A_T) for the TMDSC experiment becomes crucial, and quite often is not easily selected until rather more is already known about the sample response.

In the light of these experimental difficulties it is perhaps evident why the technique of TMDSC appears to suffer from some limitations. Furthermore, after an initial burst of enthusiastic use, during which time there was an exponential growth in the number of papers reporting TMDSC data and analysis, the trend has noticeably reduced. The time has come for a more sober reflection of what it really can offer in the way of an enhanced thermal analytical performance.

References

[1] M. Reading, Trends Polymer Sci. 1 (1993) 248.
[2] H. Gobrecht, K. Hamann, G. Willers, J. Phys. E, Sci. Instrum. 4 (1971) 21.
[3] J.E.K. Schawe, G.W.H. Höhne, Thermochim. Acta 304/305 (1997) 111.

[4] K.J. Jones, I. Kinshott, M. Reading, A.A. Lacey, C. Nikolopoulos, H.M. Pollock, Thermochim. Acta 304/305 (1997) 187.
[5] S.M. Sarge, G.W.H. Höhne, H.K. Cammenga, W. Eysel, E. Gmelin, Thermochim. Acta 361 (2000) 1.
[6] V.B.F. Mathot, in: V.B.F. Mathot (Ed.), Calorimetry and Thermal Analysis of Polymers, Carl Hanser Verlag, Munich, 1994, Chapter 5, pp. 105–167.
[7] M. Alsleben, C. Schick, W. Mischok, Thermochim. Acta 187 (1991) 261.
[8] B. Wunderlich, A. Boller, I. Okazaki, S. Kreitmeier, Thermochim. Acta 282/283 (1996) 143.
[9] T. Ozawa, K. Kanari, Thermochim. Acta 288 (1996) 39.
[10] J.E.K. Schawe, W. Winter, Thermochim. Acta 298 (1997) 9.
[11] B. Schenker, F. Stäger, Thermochim. Acta 304/305 (1997) 219.
[12] S. Weyer, A. Hensel, C. Schick, Thermochim. Acta 304/305 (1997) 267.
[13] B. Schenker, G. Widmann, R. Riesen, J. Thermal Anal. 49 (1997) 1097.
[14] T. Ozawa, K. Kanari, J. Thermal Anal. Calorim. 54 (1998) 521.
[15] Z. Jiang, C.T. Imrie, J.M. Hutchinson, Thermochim. Acta 315 (1998) 1.
[16] Z. Jiang, C.T. Imrie, J.M. Hutchinson, Thermochim. Acta 336 (1999) 27.
[17] Z. Jiang, C.T. Imrie, J.M. Hutchinson, J. Thermal Anal. Calorim. 64 (2001) 85.
[18] M. Merzlyakov, C. Schick, Thermochim. Acta 330 (1999) 55.
[19] Y-H. Jeong, Thermochim. Acta 304/305 (1997) 67.
[20] J.E.K. Schawe, Thermochim. Acta 304/305 (1997) 111.
[21] E. Donth, J. Korus, E. Hempel, M. Beiner, Thermochim. Acta 304/305 (1997) 239.
[22] G.W.H. Höhne, Thermochim. Acta 304/305 (1997) 121.
[23] J.M. Hutchinson, S. Montserrat, Thermochim. Acta 304/305 (1997) 257.